Letter

Transport and entanglement growth in long-range random Clifford circuits

Jonas Richter[1,2,3] Oliver Lunt[4,5] and Arijeet Pal[1]

[1]*Department of Physics and Astronomy, University College London, Gower Street, London WC1E 6BT, United Kingdom*
[2]*Department of Physics, Stanford University, Stanford, California 94305, USA*
[3]*Institut für Theoretische Physik, Leibniz Universität Hannover, Appelstraße 2, 30167 Hannover, Germany*
[4]*Department of Physics, King's College London, Strand, London WC2R 2LS, United Kingdom*
[5]*School of Physics and Astronomy, University of Birmingham, Birmingham B15 2TT, United Kingdom*

(Received 30 May 2022; accepted 3 February 2023; published 3 March 2023)

Conservation laws can constrain entanglement dynamics in isolated quantum systems, manifest in a slowdown of higher Rényi entropies. Here, we explore this phenomenon in a class of long-range random Clifford circuits with $U(1)$ symmetry where transport can be tuned from diffusive to superdiffusive. We unveil that the different hydrodynamic regimes reflect themselves in the asymptotic entanglement growth according to $S(t) \propto t^{1/z}$ where the dynamical transport exponent z depends on the probability $\propto r^{-\alpha}$ of gates spanning a distance r. For sufficiently small α, we show that the presence of hydrodynamic modes becomes irrelevant such that $S(t)$ behaves similarly in circuits with and without conservation law. We explain our findings in terms of the inhibited operator spreading in $U(1)$-symmetric Clifford circuits where the emerging light cones can be understood in the context of classical Lévy flights. Our Letter sheds light on the connections between Clifford circuits and more generic many-body quantum dynamics.

DOI: 10.1103/PhysRevResearch.5.L012031

Introduction. Fundamental questions on the origin of quantum statistical mechanics have experienced a renaissance in recent years [1–3] with experiments being able to probe chaos and information scrambling [4–7]. While much progress has been made due to sophisticated numerical methods (e.g., Refs. [8–13]), ideas from quantum information provide a useful lens on quantum dynamics far from equilibrium. In particular, suitable random-circuit models capture aspects of generic quantum systems [14–17], including settings with conservation laws and constraints [18–20], as well as dual unitary [21,22], time periodic [23,24], or nonunitary dynamics [25,26]. Random circuits are particularly attractive in view of today's noisy intermediate-scale quantum devices [27–29] with applications in achieving a quantum computational advantage [30] and exploring operator entanglement [31].

In the case of chaotic quantum systems with short-ranged interactions, conservation laws give rise to hydrodynamic modes that typically decay diffusively [32–35], whereas entanglement is expected to grow ballistically [36]. Remarkably, recent work unveiled that this picture is incomplete and that transport and entanglement are intimately connected [37–41]. Specifically, diffusive transport can constrain higher Rényi entropies to increase diffusively [37],

$$S_{n>1}(t) \propto \sqrt{t}, \quad \text{where } S_n = \log_2 \mathrm{tr}\left[\rho_A^n\right]/(1-n), \qquad (1)$$

with $\rho_A = \mathrm{tr}_B\, |\psi(t)\rangle\langle\psi(t)|$ denoting the reduced density matrix for a bipartition into subsystems A and B, and $|\psi(t)\rangle$ is the state of the system. In contrast, the von Neumann entropy $S_1 = -\mathrm{tr}[\rho_A \log_2 \rho_A]$ grows linearly as usual, $S_1(t) \propto t$. In this Letter, we demonstrate that constrained entanglement dynamics occurs more generically also for other transport types, and can be readily explored in $U(1)$-symmetric long-range Clifford circuits [Fig. 1(a)]. Depending on the probability $\propto r^{-\alpha}$ of gates spanning a distance r, the emerging transport can be tuned from diffusive to superdiffusive. These circuits can be seen as minimal models to describe the scrambling dynamics of long-range Hamiltonian systems. Specifically, it was found in Refs. [42,43] that the light-cone spreading in such circuits is very similar to the dynamics generated by Hamiltonians with interactions decaying as $\propto r^{-\alpha'}$, where $\alpha' = \alpha/2$. Although Clifford gates are insufficient for universal quantum computation, they form unitary 2-designs [44] (3-designs for qubits [45]) such that circuit averages of certain quantities, e.g., out-of-time-ordered correlators, coincide with Haar averages over the full unitary group [15,16]. Clifford circuits can, thus, be useful to study aspects of more generic quantum dynamics.

Long-range interactions are ubiquitous in nature, including dipolar or van der Waals interactions [46], experimentally realized in various platforms [47–53]. In contrast to short-range models where Lieb-Robinson bounds confine correlations to a linear light cone [54], long-range interactions may lead to faster information propagation [55,56]. Much effort has been invested to tighten Lieb-Robinson-like bounds for power-law interacting models [42,57–67] and to study transport and entanglement dynamics [43,68–77]. For chaotic systems in d dimensions, it was argued that linear light cones arise for $\alpha' > d + 1/2$ with properties similar to short-range models,

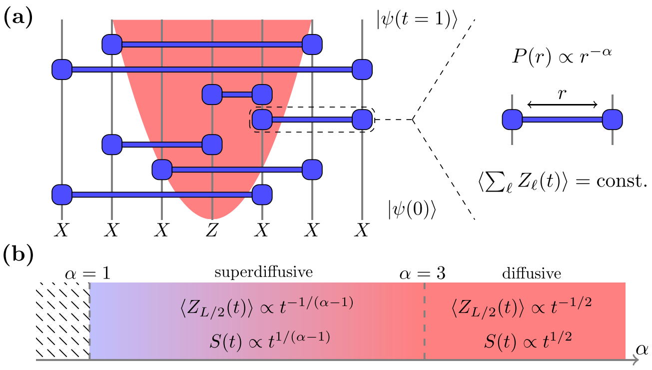

FIG. 1. (a) Two-qubit Clifford gates of range r occur with probability $P(r) \propto r^{-\alpha}$ and conserve the total Pauli-Z component, see Supplemental Material [92] for more details. (b) By tuning $\alpha > 1$, different hydrodynamic regimes with dynamical exponent z [Eq. (2)] emerge, manifest in the tails of the circuit-averaged expectation value $\langle Z_{L/2}(t) \rangle \propto t^{-1/z}$. Entanglement saturates approximately on a timescale $\propto L^z$, implying that it asymptotically mirrors the transport behavior, $S(t) \propto t^{1/z}$.

whereas power-law or logarithmic bounds emerge for $d/2 < \alpha' < d + 1/2$ [42,64]. For $\alpha' < d/2$, locality breaks down, and information propagation becomes essentially instantaneous [78].

From a numerical point of view, long-range systems are challenging due to quick entanglement generation and strong finite-size effects [79]. In contrast, the random Clifford circuits considered here can be simulated efficiently even for large systems. Summarizing our main results, we unveil a direct correspondence between transport and entanglement with entanglement saturating on a timescale $t_{\text{sat}} \propto L^z$ implying an asymptotic scaling $S(t) \propto t^{1/z}$, where z is the dynamical transport exponent [Fig. 1(b)]. We explain this finding in terms of the inhibited operator spreading in $U(1)$-symmetric Clifford circuits, leading to narrower light cones compared to circuits without conservation law. Moreover, we demonstrate that the constraint on $S(t)$ becomes insignificant once the dynamical exponent for transport reaches $z \approx 1$.

Clifford circuits with symmetry. Clifford circuits are of major interest in quantum information [80], including error correction and randomized benchmarking [81,82]. In the context of quantum dynamics, they recently gained popularity to study measurement-induced entanglement transitions (e.g., Refs. [43,83–87]) as their efficient simulability allows to access large system sizes [88,89]. The key idea is to exploit the stabilizer formalism [80,90], where a state $|\psi\rangle$ on L qubits can be uniquely defined by L operators O_i, i.e., $O_i |\psi\rangle = |\psi\rangle$, where $O_i = X_1^{\nu_1^i} Z_1^{\mu_1^i} \cdots X_\ell^{\nu_\ell^i} Z_\ell^{\mu_\ell^i} \cdots X_L^{\nu_L^i} Z_L^{\mu_L^i}$ are L-site Pauli strings and $\nu_\ell^i, \mu_\ell^i = \{0, 1\}$ [88]. Since Clifford gates preserve the Pauli group, the action $|\psi\rangle \to \mathcal{U} |\psi\rangle$ of a Clifford gate $\mathcal{U}$ can be efficiently described by the stabilizers, $\mathcal{U} O_i \mathcal{U}^\dagger$ [91], e.g., by storing the ν_ℓ^i, μ_ℓ^i in a binary matrix $\mathcal{M}$ and updating their values appropriately [88].

We show that random Clifford circuits can elucidate the interplay between transport and entanglement [39]. We consider circuits with $U(1)$ symmetry where one time step is defined as the application of L gates conserving the total magnetization, $\langle \psi(t)| \sum_\ell Z_\ell |\psi(t)\rangle = \text{const.}$ (Fig. 1). This property is quite restrictive: Although the full two-qubit Clifford group has 11520 distinct elements (modulo a global phase), only 64 conserve the total Pauli-Z component, see Ref. [92]. Due to the $U(1)$ symmetry and the Pauli-preserving property of Clifford gates, it turns out that transport can be understood classically in terms of long-range random walks, so-called Lévy flights [53,69,95,96]. However, we will show that such constrained circuits still generate extensive entanglement, similar to Haar-random circuits [14].

Product states such as $|{\rightarrow}\rangle^{\otimes L}$ with spins in the x direction can be stabilized by operators $O_i = X_i$ $(i = 1, \ldots, L)$ acting nontrivially only on a single site. Evolving $|\psi\rangle$ with respect to a random circuit will cause the O_i to become nonlocal, resulting in increased entanglement. Clifford circuits are special as they generate flat entanglement spectra such that all S_n's are equivalent [97]. Although the different behaviors of S_1 and $S_{n>1}$ demonstrated in Ref. [37], therefore, cannot be resolved, $S(t)$ is, nevertheless, sensitive to conservation laws, and $S(t) \propto \sqrt{t}$ was found in Clifford circuits with diffusive transport [39]. Here, we show that long-range circuits provide an ideal framework to study entanglement dynamics also for other transport types. To this end, we reiterate the arguments to explain the constrained entanglement growth [37,38]: Consider the reduced density matrix ρ_A with χ nonzero eigenvalues $\Lambda_1 \leqslant \cdots \leqslant \Lambda_\chi$. In the presence of hydrodynamic modes with dynamical exponent z, Λ_χ can be bounded by $\Lambda_\chi \gtrsim e^{-\gamma t^{1/z}}$ with some constant γ, where $z = 2$ corresponds to diffusion [37,38]. The bound results from rare contributions to $|\psi(t)\rangle$ where a region of length ξ around the cut between A and B is in the $|{\uparrow}\rangle$ state, acting as a bottleneck for entanglement as it takes time $\propto \xi^z$ for a $|{\downarrow}\rangle$ to get across the cut. It follows that $S_{n\to\infty} = -\log_2 \Lambda_\chi$ scales as $S_\infty(t) \propto t^{1/z}$ and due to $S_\infty \leqslant S_{n>1} \leqslant n S_\infty/(n-1)$, all $S_{n>1}(t)$'s obey this scaling. This is independent of the type of time evolution and generalizes to Clifford circuits, where $\Lambda_i = \Lambda$ and $S_n(t) \equiv S(t)$.

Hydrodynamics. By varying α, it is possible to tune the nature of transport. Consider a state $|\psi\rangle = |{\rightarrow}\rangle^{\otimes L/2-1} |{\uparrow}\rangle |{\rightarrow}\rangle^{\otimes L/2}$, stabilized by X_ℓ for $\ell \neq L/2$, and Z_ℓ for $\ell = L/2$, cf. Fig. 1(a). The action $\mathcal{U} O_i \mathcal{U}^\dagger$ of $U(1)$-symmetric Clifford gates on the two classes of stabilizers is quite different. While X_ℓ becomes nonlocal and generates entanglement, the stabilizer $Z_{L/2}$ remains of length one throughout the circuit [92]. Specifically, the Z operator performs α-dependent random walks, i.e., Lévy flights [53,69], examples of which are shown in Figs. 2(a) and 2(b) for $\alpha = 5$ and $\alpha = 2$. Consequently, at a given time, there will be a site ℓ with $\langle \psi(t)|Z_\ell|\psi(t)\rangle = 1$ unentangled with the rest of the system [98].

Simulating 1d circuits with $L = 1024$, Figs. 2(a) and 2(b) show the circuit-averaged value $\langle Z_\ell(t)\rangle$ for $\sim 10^5$ random realizations of $\mathcal{U} Z_{L/2} \mathcal{U}^\dagger$, highlighting a change from local to nonlocal when reducing α. Analyzing $\langle Z_\ell(t)\rangle$ at fixed t, we find Gaussian profiles for $\alpha = 5$ that collapse when rescaled appropriately [Fig. 2(c)], indicating diffusion. In contrast, $\langle Z_\ell(t)\rangle$ is non-Gaussian for $\alpha = 2$ but rather described by a Lorentzian, signaling superdiffusive transport [68,69]. (See Ref. [92] for other α and 2d circuits.) The α-dependent transport regimes are also reflected in the decay at $\ell = L/2$, $\langle Z_{L/2}(t)\rangle \propto t^{-1/z}$, where z approximately follows the Lévy-

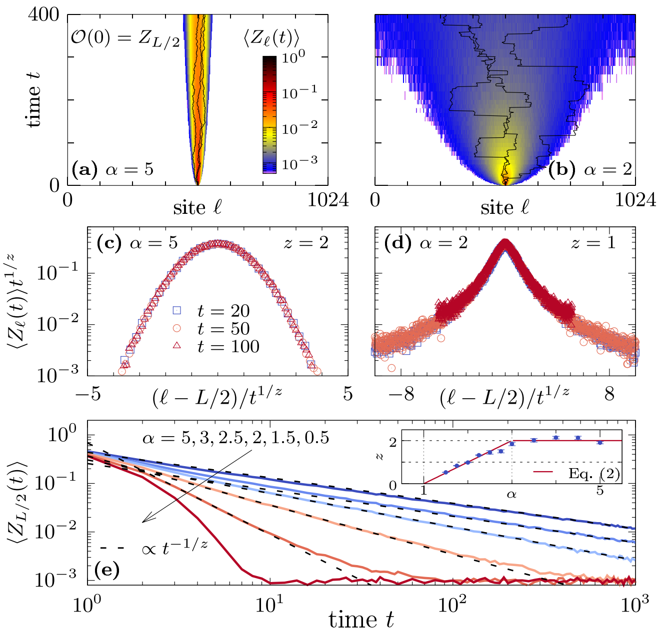

FIG. 2. [(a) and (b)] $\langle Z_\ell(t)\rangle$ averaged over $\sim 10^5$ circuit realizations for $\alpha = 5$, $\alpha = 2$, and $L = 1024$. Solid curves indicate individual realizations, i.e., random walks with step-size distribution $\propto r^{-\alpha}$. [(c) and (d)] $\langle Z_\ell(t)\rangle t^{1/z}$ at fixed t, plotted against $(\ell - L/2)/t^{1/z}$. (e) $\langle Z_{L/2}(t)\rangle$ for different α. Dashed lines indicate power-law $\propto t^{-1/z}$. The inset shows z extracted from the fits and compared to Eq. (2).

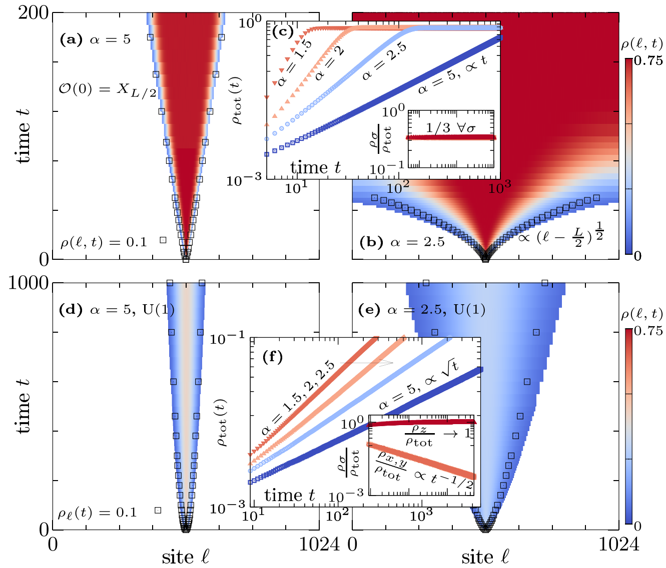

FIG. 3. [(a) and (b)] Averaged $\rho(\ell, t)$ in full Clifford circuits with $\alpha = 5$ and $\alpha = 2.5$, obtained from $O(0) = X_{L/2}$ with $L = 1024$. Symbols indicate $\rho(\ell, t) = 10^{-1}$. (c) $\rho_{\rm tot}(t)$ for $L = 2048$ and different α's (see also Ref. [92]). The inset shows $\rho_\sigma(t)/\rho_{\rm tot}(t) \approx 1/3$, i.e., all Σ^σ's contribute equally. [(d)–(f)] Analogous data but for $U(1)$-symmetric circuits, where $O(t)$ spreads significantly slower. This stems from the dominant contribution of Z operators within $\rho_{\rm tot}(t)$, cf. inset in (f) for $\alpha = 5$.

flight prediction [53,69,99],

$$z = \begin{cases} 2, & \alpha \geqslant 3; \\ \alpha - 1, & 1 < \alpha \leqslant 3, \end{cases} \tag{2}$$

with no hydrodynamic tail for $\alpha \leqslant 1$ [Fig. 2(e)]. Clifford and $U(1)$-symmetric Haar-random gates are expected to yield the same circuit-averaged $\langle Z_\ell(t)\rangle$. In contrast, individual circuit realizations differ since Haar gates distribute the Z excitation smoothly over multiple sites whereas Clifford gates yield sharp random walks. The transport behavior in Fig. 2 agrees qualitatively with the emergent quantum hydrodynamics observed in long-range Hamiltonian systems [53,69]. Even though transport in the Clifford case is a purely classical process, the average coarse-grained type of hydrodynamics, both in the circuit and the Hamiltonian model, is especially at high temperatures mainly set by the range of the interactions (i.e., by α), and not so much by the microscopic dynamics.

Operator spreading. While $\mathcal{U}Z_\ell\mathcal{U}^\dagger$ remains a single-site operator for $U(1)$-symmetric Clifford gates (Fig. 2), we now consider $O = X_\ell$. Generally, $O(t) = \sum_{\mathcal{S}} \alpha_{\mathcal{S}}(t)\mathcal{S}$ can be written in the basis of the 4^L Pauli strings $\mathcal{S}$. Evolution under Haar-random gates increases the number of nonzero $\alpha_{\mathcal{S}}(t)$ [14–16], leading to operator entanglement [100]. In contrast, Clifford gates map Pauli operators to each other, $O(t) = \delta_{\mathcal{S},O(t)}\mathcal{S}$ with no operator entanglement. However, $O(t)$ will become nonlocal, manifested by its growing support $\rho_{\rm tot}(t) = \frac{1}{L}\sum_{\ell,\sigma} \rho_\sigma(\ell, t)$, where $\rho_\sigma(\ell, t) = {\rm tr}[O_\ell(t)\Sigma^\sigma]/2$, $O_\ell(t)$ is the matrix at position ℓ in the string, and $\Sigma^\sigma = \{X, Y, Z\}$, $\sigma = x, y, z$.

Considering $O(0) = X_{L/2}$, we plot $\rho(\ell, t) = \sum_\sigma \rho_\sigma(\ell, t)$ in Fig. 3, which is a measure for the out-of-time-ordered correlator between operators at sites ℓ and $L/2$ [101]. For circuits without conservation law [Figs. 3(a) and 3(b)], we observe a linear light cone for $\alpha = 5$, whereas a power-law light cone emerges for $\alpha = 2.5$, in agreement with the phase diagram in Ref. [42]. Correspondingly, we find $\rho_{\rm tot}(t) \propto t$ at $\alpha = 5$ and faster growth for smaller α [Fig. 3(c)], see also Ref. [92]. In the bulk of the light cone, we observe full scrambling with $\rho(\ell, t) \to 3/4$ and $\rho_\sigma(t)/\rho_{\rm tot}(t) \approx 1/3$ [insets in Fig. 3(c)], where $\rho_\sigma(t) = \sum_\ell \rho_\sigma(\ell, t)$ is the Pauli-component resolved support. Speaking differently, the interior of the light cone has reached an equilibrium distribution where local X, Y, Z operators are equally likely. We will discuss the dynamics of the light-cone edges further below in the context of Fig. 4.

Next, turning to $U(1)$-symmetric gates, the behavior of $\rho(\ell, t)$ changes drastically [Figs. 3(d) and 3(e)]. Namely, operator spreading is significantly slower and resembles the transport behavior of the conserved quantity [Eq. (2)], with a diffusive (superdiffusive) light cone for $\alpha = 5$ ($\alpha = 2.5$), also reflected in the growth of $\rho_{\rm tot}(t)$ [Fig. 3(f)]. This is due to the properties of the $U(1)$-symmetric Clifford gates, which cause $O(t)$ to be dominated by Z operators. Given the initial operator $O(0) = X_{L/2}$ with a single X at $\ell = L/2$ and identity operators on all other sites, it is, in fact, significantly more likely that a random gate will generate more Z than X, Y operators and thereby increase the overall share of Z in $O(t)$, see Ref. [92] for details. This is shown in the inset of Fig. 3(f) for $\alpha = 5$ where we find $\rho_z(t) \propto t^{1/2}$ whereas $\rho_{x,y}(t) = {\rm const.}$ such that $\rho_z(t)/\rho_{\rm tot}(t) \to 1$. The inhomogeneous composition of $O(t)$ differs from the unsymmetric case where X, Y, and Z

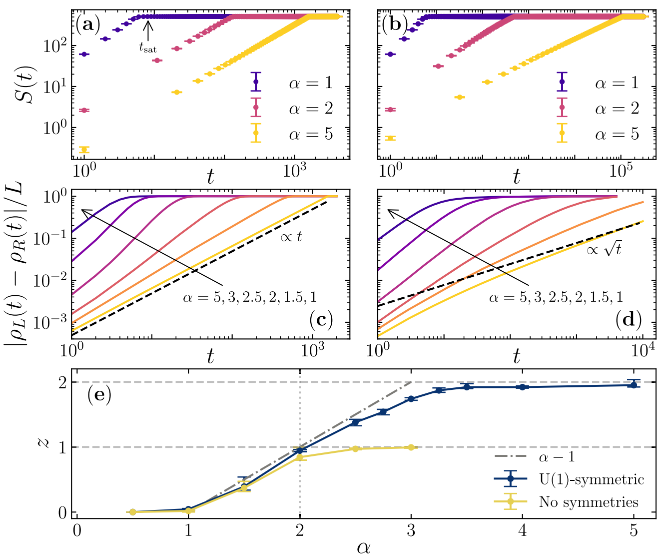

FIG. 4. [(a) and (b)] $S(t)$ for different α's in asymmetric and $U(1)$-symmetric circuits with $L = 1024$ and open boundaries. For $\alpha \geqslant 3$, we expect short-range behavior: $z = 2$ with $U(1)$ symmetry and $z = 1$ without. [(c) and(d)] Normalized difference between left (right) endpoints of $O(t)$ for $L = 2048$. The dashed curves indicate $\propto t$ ($\propto \sqrt{t}$) scaling. (e) z versus α for circuits with and without conservation law. The deviations from Eq. (2) around $\alpha = 3$ may be due to logarithmic corrections to transport [69].

occur with equal probability [Fig. 3(c)]. The large fraction of Z operators behaves similarly to Fig. 2, leading to narrower light cones compared to circuits without conservation law. Furthermore, studying the bulk of the light cone, we find that $\rho(\ell, t) < 3/4$ in the $U(1)$-symmetric case [Figs. 3(d) and 3(e)]. This indicates that, at least, on the timescales shown here, the operator string is not fully scrambled and contains, on average, more identity operators than in the case without conservation law.

The operator spreading in $U(1)$-symmetric Clifford circuits is notably simpler compared to the Haar-random case where the conserved charges lag behind the light-cone front which propagates quickly due to nonconserved operators [18]. Although Clifford gates fail to capture this aspect of generic quantum dynamics, the simplified description is helpful to understand the constrained entanglement dynamics since the light cones in Fig. 3 upper bound the growth of $S(t)$ [14].

Entanglement dynamics. Choosing $|\psi(0)\rangle = |\rightarrow\rangle^{\otimes L}$, we study $S(t) = \text{rank}(\mathcal{M}_{L/2}) - L/2$ for a half-system cut, where $\mathcal{M}_{L/2}$ denotes the stabilizer matrix of the first $L/2$ sites [14,102,103]. From this expression, it is clear that $S(t)$ depends on the collective dynamics of $|\psi(t)\rangle$'s stabilizers. Since $|\psi(0)\rangle$ is a superposition of all symmetry sectors, $S(t \to \infty) \approx L/2$ saturates at the same value in circuits with and without the conservation law [Figs. 4(a) and 4(b)]. We find it convenient to analyze the α dependence of $S(t)$ by extracting the saturation time $t_{\text{sat}} \propto L^z$ for different L's, implying an asymptotic scaling $S(t) \propto t^{1/z}$. The obtained values of z are summarized in Fig. 4(e). In the case of $U(1)$-symmetric circuits, we find that the transport behavior is reflected in the entanglement dynamics, and z is reasonably well described by Eq. (2). In addition, whereas we recover $z \to 1$ in unsymmetric circuits for $\alpha \geqslant 3$ as expected for short-range models [14], the scaling behaviors of circuits with and without conservation law become similar for $\alpha \lesssim 2$ with all discrepancies in z estimates contained within error bars.

At small α, transport is fast enough that entanglement growth is mainly dictated by the gate range and not by the conservation law. Specifically, at $\alpha = 2$ we have $z \approx 1$ and the bound $\Lambda_\chi \gtrsim e^{-\gamma t^{1/z}}$ due to transport becomes comparable to the typical value $\sim e^{-\gamma t}$ expected given the ballistic $S_1(t)$ in generic circuits [37]. The behavior of the edges of the light cone can provide further quantitative insights. Specifically, we study the end points $\rho_{L(R)}(t)$ of a string $O(t)$, i.e., the left(right)most ℓ where $O_\ell(t)$ is nonidentity. Once a nontrivial part of $O(t)$ extends across the cut, entanglement may, in principle, increase. One might, therefore, expect that $\rho_{L(R)}(t)$ is more relevant for $S(t)$ than $\rho_{\text{tot}}(t)$ [Fig. 3]. As shown in Figs. 4(c) and 4(d), we find that $|\rho_L(t) - \rho_R(t)|/L$ behaves very differently in symmetric and unsymmetric circuits for $\alpha = 5$ but grows with roughly comparable rate if α is small (see also Ref. [92]), which is consistent with the observed similar growth rate of entanglement.

We expect the relation between transport and entanglement to carry over to Rényi entropies $S_{n>1}(t)$ in generic systems with a conserved quantity, see Ref. [92] for some evidence in a long-range tilted field Ising model. Since Clifford gates form unitary 3-designs [44,45], they give the same "annealed" Rényi-2 entropy $S_2^{(a)} = -\log_2 \overline{\text{tr}_A \rho_A^2}$ as a Haar-random circuit. Although $S_2^{(a)} \leqslant \overline{S_2}$ only lower bounds the average $\overline{S_2}$, in $U(1)$-symmetric Haar-random circuits it displays the same $\sqrt{t}$ growth as $\overline{S_2}$ [37], consistent with small sample-to-sample fluctuations of $S_2(t)$.

Let us comment on the deviations in Fig. 4(e) from the prediction (2), most pronounced near $\alpha = 3$. Even for $L \sim 10^3$ presented here, we observe a drift of z with L. We attempt to account for these finite-size effects by restricting the data to $L \leqslant L_{\text{end}}$ and extrapolating $z(L_{\text{end}})$ to $1/L_{\text{end}} \to 0$. For details, including how we obtain the error bars, see Ref. [92]. Precisely at $\alpha = 3$, transport can receive logarithmic corrections [69], which may also explain the faster entanglement growth. Repeating our analysis but with $S(t) \sim t^{1/z}\sqrt{\log t}$, we obtain $z = 1.91(1)$ much closer to $z = 2$ [104]. The marginality at $\alpha \approx 3$ is also reflected in the development of non-Gaussian tails in both $\langle Z_\ell(t)\rangle$ and $\rho(\ell, t)$ [92].

Conclusion. We have studied the interplay of transport and entanglement dynamics in long-range random Clifford circuits with $U(1)$ symmetry. We demonstrated that the emerging transport regimes with dynamical exponent z reflect themselves in the growth of entanglement as $S(t) \propto t^{1/z}$, generalizing earlier work that has focused on diffusive systems with $z = 2$ [37]. Although we expect this result to hold also in more generic Haar-random circuits or chaotic quantum systems for $S_{n>1}(t)$, we here provided a simplified picture specific to the Clifford framework where operator strings become dominated by the conserved quantity leading to narrower light cones. Although transport in Clifford circuits turned out to be purely classical, their efficient simulability may suggest the study of possible connections with recent state-of-the-art methods to capture transport coefficients [10–12,105–108] and to better understand the role of entanglement and the differences to full thermalizing quantum dynamics [109].

A promising research direction is to consider entanglement dynamics in Clifford circuits with other gate sets or conservation laws, potentially giving rise to localization [110] as well as adding measurements which can induce nonequilibrium phases in circuits with symmetry [111,112]. Studying the impact of sporadic non-Clifford gates, acting as seeds of chaos [113], is another natural avenue. Finally, it would be interesting if the transport-dependent entanglement growth is observable in quantum-simulator experiments where diffusion and superdiffusion can be realized [53,114], and the Rényi-2 entropy is accessible for small systems [115,116].

Acknowledgments. We sincerely thank L. Masanes for a helpful comment. This work was funded by the European Research Council (ERC) under the European Union's Horizon 2020 Research and Innovation Programme (Grant Agreement No. 853368). J.R. also received funding from the European Union's Horizon Europe Programme under the Marie Skłodowska-Curie Grant Agreement No. 101060162. O.L. acknowledges support by UK Research and Innovation (UKRI) (Grant No. MR/T040947/1).

---

[1] L. D'Alessio, Y. Kafri, A. Polkovnikov, and M. Rigol, From quantum chaos and eigenstate thermalization to statistical mechanics and thermodynamics, Adv. Phys. **65**, 239 (2016).

[2] R. Nandkishore and D. A. Huse, Many-body localization and thermalization in quantum statistical mechanics, Annu. Rev. Condens. Matter Phys. **6**, 15 (2015).

[3] B. Bertini, F. Heidrich-Meisner, C. Karrasch, T. Prosen, R. Steinigeweg, and M. Žnidarič, Finite-temperature transport in one-dimensional quantum lattice models, Rev. Mod. Phys. **93**, 025003 (2021).

[4] J. Li, R. Fan, H. Wang, B. Ye, B. Zeng, H. Zhai, X. Peng, and J. Du, Measuring Out-of-Time-Order Correlators on a Nuclear Magnetic Resonance Quantum Simulator, Phys. Rev. X **7**, 031011 (2017).

[5] M. Gärttner, J. G. Bohnet, A. Safavi-Naini, M. L. Wall, J. J. Bollinger, and A. M. Rey, Measuring out-of-time-order correlations and multiple quantum spectra in a trapped ion quantum magnet, Nat. Phys. **13**, 781 (2017).

[6] K. A. Landsman, C. Figgatt, T. Schuster, N. M. Linke, B. Yoshida, N. Y. Yao, and C. Monroe, Verified quantum information scrambling, Nature (London) **567**, 61 (2019).

[7] M. S. Blok, V. V. Ramasesh, T. Schuster, K. O'Brien, J. M. Kreikebaum, D. Dahlen, A. Morvan, B. Yoshida, N. Y. Yao, and I. Siddiqi, Quantum Information Scrambling on a Superconducting Qutrit Processor, Phys. Rev. X **11**, 021010 (2021).

[8] J. Haegeman, J. I. Cirac, T. J. Osborne, I. Pižorn, H. Verschelde, and F. Verstraete, Time-Dependent Variational Principle for Quantum Lattices, Phys. Rev. Lett. **107**, 070601 (2011).

[9] S. Paeckel, T. Köhler, A. Swoboda, S. R. Manmana, U. Schollwöck, and C. Hubig, Time-evolution methods for matrix-product states, Ann. Phys. (NY) **411**, 167998 (2019).

[10] T. Rakovszky, C. W. von Keyserlingk, and F. Pollmann, Dissipation-assisted operator evolution method for capturing hydrodynamic transport, Phys. Rev. B **105**, 075131 (2022).

[11] C. D. White, M. Zaletel, R. S. K. Mong, and G. Refael, Quantum dynamics of thermalizing systems, Phys. Rev. B **97**, 035127 (2018).

[12] J. Wurtz, A. Polkovnikov, and D. Sels, Cluster truncated Wigner approximation in strongly interacting systems, Ann. Phys. (NY) **395**, 341 (2018).

[13] T. Heitmann, J. Richter, D. Schubert, and R. Steinigeweg, Selected applications of typicality to real-time dynamics of quantum many-body systems, Z. Naturforsch., A: Phys. Sci. **75**, 421 (2020).

[14] A. Nahum, J. Ruhman, S. Vijay, and J. Haah, Quantum Entanglement Growth under Random Unitary Dynamics, Phys. Rev. X **7**, 031016 (2017).

[15] C. W. von Keyserlingk, T. Rakovszky, F. Pollmann, and S. L. Sondhi, Operator Hydrodynamics, OTOCs, and Entanglement Growth in Systems without Conservation Laws, Phys. Rev. X **8**, 021013 (2018).

[16] A. Nahum, S. Vijay, and J. Haah, Operator Spreading in Random Unitary Circuits, Phys. Rev. X **8**, 021014 (2018).

[17] F. G. S. L. Brandão, W. Chemissany, N. Hunter-Jones, R. Kueng, and J. Preskill, Models of quantum complexity growth, PRX Quantum **2**, 030316 (2021).

[18] V. Khemani, A. Vishwanath, and D. A. Huse, Operator Spreading and the Emergence of Dissipative Hydrodynamics under Unitary Evolution with Conservation Laws, Phys. Rev. X **8**, 031057 (2018).

[19] T. Rakovszky, F. Pollmann, and C. W. von Keyserlingk, Diffusive Hydrodynamics of Out-of-Time-Ordered Correlators with Charge Conservation, Phys. Rev. X **8**, 031058 (2018).

[20] S. Moudgalya, A. Prem, D. A. Huse, and A. Chan, Spectral statistics in constrained many-body quantum chaotic systems, Phys. Rev. Res. **3**, 023176 (2021).

[21] B. Bertini, P. Kos, and T. Prosen, Exact Correlation Functions for Dual-Unitary Lattice Models in $1+1$ Dimensions, Phys. Rev. Lett. **123**, 210601 (2019).

[22] P. W. Claeys and A. Lamacraft, Ergodic and Nonergodic Dual-Unitary Quantum Circuits with Arbitrary Local Hilbert Space Dimension, Phys. Rev. Lett. **126**, 100603 (2021).

[23] B. Bertini, P. Kos, and T. Prosen, Exact Spectral Form Factor in a Minimal Model of Many-Body Quantum Chaos, Phys. Rev. Lett. **121**, 264101 (2018).

[24] A. Chan, A. De Luca, and J. T. Chalker, Spectral Statistics in Spatially Extended Chaotic Quantum Many-Body Systems, Phys. Rev. Lett. **121**, 060601 (2018).

[25] B. Skinner, J. Ruhmann, and A. Nahum, Measurement-Induced Phase Transitions in the Dynamics of Entanglement, Phys. Rev. X **9**, 031009 (2019).

[26] A. C. Potter and R. Vasseur, in *Entanglement Dynamics in Hybrid Quantum Circuits*, edited by A. Bayat, S. Bose, and H. Johannesson, Quantum Science and Technology (Springer, Cham, 2022).

[27] J. Preskill, Quantum computing in the NISQ era and beyond, Quantum **2**, 79 (2018).

[28] J. Richter and A. Pal, Simulating Hydrodynamics on Noisy Intermediate-Scale Quantum Devices with Random Circuits, Phys. Rev. Lett. **126**, 230501 (2021).

[29] O. Lunt, J. Richter, and A. Pal, in *Quantum Simulation Using Noisy Unitary Circuits and Measurements*, edited by A. Bayat, S. Bose, and H. Johannesson, Entanglement in Spin Chains. Quantum Science and Technology (Springer, Cham, 2022).

[30] F. Arute *et al.*, Quantum supremacy using a programmable superconducting processor, Nature (London) **574**, 505 (2019).

[31] X. Mi *et al.*, Information scrambling in quantum circuits, Science **374**, 1479 (2021).

[32] J. Lux, J. Müller, A. Mitra, and A. Rosch, Hydrodynamic long-time tails after a quantum quench, Phys. Rev. A **89**, 053608 (2014).

[33] A. Bohrdt, C. B. Mendl, M. Endres, and M. Knap, Scrambling and thermalization in a diffusive quantum many-body system, New J. Phys. **19**, 063001 (2017).

[34] J. Richter, F. Jin, H. De Raedt, K. Michielsen, J. Gemmer, and R. Steinigeweg, Real-time dynamics of typical and untypical states in nonintegrable systems, Phys. Rev. B **97**, 174430 (2018).

[35] J. Richter, F. Jin, L. Knipschild, J. Herbrych, H. De Raedt, K. Michielsen, J. Gemmer, and R. Steinigeweg, Magnetization and energy dynamics in spin ladders: Evidence of diffusion in time, frequency, position, and momentum, Phys. Rev. B **99**, 144422 (2019).

[36] H. Kim and D. A. Huse, Ballistic Spreading of Entanglement in a Diffusive Nonintegrable System, Phys. Rev. Lett. **111**, 127205 (2013).

[37] T. Rakovszky, F. Pollmann, and C. W. von Keyserlingk, Subballistic Growth of Rényi Entropies due to Diffusion, Phys. Rev. Lett. **122**, 250602 (2019).

[38] Y. Huang, Dynamics of Rényi entanglement entropy in diffusive qudit systems, IOP SciNotes **1**, 035205 (2020).

[39] M. Žnidarič, Entanglement growth in diffusive systems, Commun. Phys. **3**, 100 (2020).

[40] T. Rakovszky, F. Pollmann, and C. von Keyserlingk, Entanglement growth in diffusive systems with large spin, Commun. Phys. **4**, 91 (2021).

[41] T. Zhou and A. W. W. Ludwig, Diffusive scaling of Rényi entanglement entropy, Phys. Rev. Res. **2**, 033020 (2020).

[42] T. Zhou, S. Xu, X. Chen, A. Guo, and B. Swingle, Operator Lévy Flight: Light Cones in Chaotic Long-Range Interacting Systems, Phys. Rev. Lett. **124**, 180601 (2020).

[43] M. Block, Y. Bao, S. Choi, E. Altman, and N. Y. Yao, Measurement-Induced Transition in Long-Range Interacting Quantum Circuits, Phys. Rev. Lett. **128**, 010604 (2022).

[44] A. W. Harrow and R. A. Low, Random quantum circuits are approximate 2-designs, Commun. Math. Phys. **291**, 257 (2009).

[45] Z. Webb, The Clifford group forms a unitary 3-design, Quantum Inf. Comput. **16**, 1379 (2016).

[46] M. Saffman, T. G. Walker, and K. Mølmer, Quantum information with Rydberg atoms, Rev. Mod. Phys. **82**, 2313 (2010).

[47] D. Porras and J. I. Cirac, Effective Quantum Spin Systems with Trapped Ions, Phys. Rev. Lett. **92**, 207901 (2004).

[48] P. Jurcevic, B. P. Lanyon, P. Hauke, C. Hempel, P. Zoller, R. Blatt, and C. F. Roos, Observation of entanglement propagation in a quantum many-body system, Nature (London) **511**, 202 (2014).

[49] J. Smith, A. Lee, P. Richerme, B. Neyenhuis, P. W. Hess, P. Hauke, M. Heyl, D. A. Huse, and C. Monroe, Many-body localization in a quantum simulator with programmable random disorder, Nat. Phys. **12**, 907 (2016).

[50] P. Richerme, Z.-X. Gong, A. Lee, C. Senko, J. Smith, M. Foss-Feig, S. Michalakis, A. V. Gorshkov, and C. Monroe, Non-local propagation of correlations in quantum systems with long-range interactions, Nature (London) **511**, 198 (2014).

[51] H. Bernien, S. Schwartz, A. Keesling, H. Levine, A. Omran, H. Pichler, S. Choi, A. S. Zibrov, M. Endres, M. Greiner, V. Vuletić, and M. D. Lukin, Probing many-body dynamics on a 51-atom quantum simulator, Nature (London) **551**, 579 (2017).

[52] A. Periwal, E. S. Cooper, P. Kunkel, J. F. Wienand, E. J. Davis, and M. Schleier-Smith, Programmable interactions and emergent geometry in an array of atom clouds, Nature (London) **600**, 630 (2021).

[53] M. K. Joshi, F. Kranzl, A. Schuckert, I. Lovas, C. Maier, R. Blatt, M. Knap, and C. F. Roos, Observing emergent hydrodynamics in a long-range quantum magnet, Science **376**, 720 (2022).

[54] E. H. Lieb and D. W. Robinson, The finite group velocity of quantum spin systems, Commun. Math. Phys. **28**, 251 (1972).

[55] N. Lashkari, D. Stanford, M. Hastings, T. Osborne, and P. Hayden, Towards the fast scrambling conjecture, J. High Energy Phys. 04 (2013) 022.

[56] M. Avellino, A. J. Fisher, and S. Bose, Quantum communication in spin systems with long-range interactions, Phys. Rev. A **74**, 012321 (2006).

[57] M. B. Hastings and T. Koma, Spectral gap and exponential decay of correlations, Commun. Math. Phys. **265**, 781 (2006).

[58] J. Eisert, M. van den Worm, S. R. Manmana, and M. Kastner, Breakdown of Quasilocality in Long-Range Quantum Lattice Models, Phys. Rev. Lett. **111**, 260401 (2013).

[59] P. Hauke and L. Tagliacozzo, Spread of Correlations in Long-Range Interacting Quantum Systems, Phys. Rev. Lett. **111**, 207202 (2013).

[60] M. Foss-Feig, Z.-X. Gong, C. W. Clark, and A. V. Gorshkov, Nearly Linear Light Cones in Long-Range Interacting Quantum Systems, Phys. Rev. Lett. **114**, 157201 (2015).

[61] M. C. Tran, A. Y. Guo, Y. Su, J. R. Garrison, Z. Eldredge, M. Foss-Feig, A. M. Childs, and A. V. Gorshkov, Locality and Digital Quantum Simulation of Power-Law Interactions, Phys. Rev. X **9**, 031006 (2019).

[62] D. J. Luitz and Y. Bar Lev, Emergent locality in systems with power-law interactions, Phys. Rev. A **99**, 010105(R) (2019).

[63] L. Colmenarez and D. J. Luitz, Lieb-Robinson bounds and out-of-time order correlators in a long-range spin chain, Phys. Rev. Res. **2**, 043047 (2020).

[64] T. Zhou and X. Chen, Operator dynamics in a Brownian quantum circuit, Phys. Rev. E **99**, 052212 (2019).

[65] T. Kuwahara and K. Saito, Strictly Linear Light Cones in Long-Range Interacting Systems of Arbitrary Dimensions, Phys. Rev. X **10**, 031010 (2020).

[66] M. C. Tran, A. Y. Guo, C. L. Baldwin, A. Ehrenberg, A. V. Gorshkov, and A. Lucas, Lieb-Robinson Light Cone for Power-Law Interactions, Phys. Rev. Lett. **127**, 160401 (2021).

[67] C.-F. Chen and A. Lucas, Optimal Frobenius light cone in spin chains with power-law interactions, Phys. Rev. A **104**, 062420 (2021).

[68] B. Kloss and Y. Bar Lev, Spin transport in a long-range-interacting spin chain, Phys. Rev. A **99**, 032114 (2019).

[69] A. Schuckert, I. Lovas, and M. Knap, Nonlocal emergent hydrodynamics in a long-range quantum spin system, Phys. Rev. B **101**, 020416(R) (2020).

[70] L. Cevolani, G. Carleo, and L. Sanchez-Palencia, Spreading of correlations in exactly solvable quantum models with long-range interactions in arbitrary dimensions, New J. Phys. **18**, 093002 (2016).

[71] T. Hashizume, S. Kuriyattil, A. J. Daley, and G. Bentsen, Tunable geometries in sparse clifford circuits, Symmetry **14**, 666 (2022).

[72] J. Schachenmayer, B. P. Lanyon, C. F. Roos, and A. J. Daley, Entanglement Growth in Quench Dynamics with Variable Range Interactions, Phys. Rev. X **3**, 031015 (2013).

[73] S. Pappalardi, A. Russomanno, B. Žunkovič, F. Iemini, A. Silva, and R. Fazio, Scrambling and entanglement spreading in long-range spin chains, Phys. Rev. B **98**, 134303 (2018).

[74] A. Lerose and S. Pappalardi, Origin of the slow growth of entanglement entropy in long-range interacting spin systems, Phys. Rev. Res. **2**, 012041(R) (2020).

[75] T. Kuwahara and K. Saito, Absence of Fast Scrambling in Thermodynamically Stable Long-Range Interacting Systems, Phys. Rev. Lett. **126**, 030604 (2021).

[76] T. Minato, K. Sugimoto, T. Kuwahara, and K. Saito, Fate of Measurement-Induced Phase Transition in Long-Range Interactions, Phys. Rev. Lett. **128**, 010603 (2022).

[77] T. Müller, S. Diehl, and M. Buchhold, Measurement-Induced Dark State Phase Transitions in Long-Ranged Fermion Systems, Phys. Rev. Lett. **128**, 010605 (2022).

[78] R. Bachelard and M. Kastner, Universal Threshold for the Dynamical Behavior of Lattice Systems with Long-Range Interactions, Phys. Rev. Lett. **110**, 170603 (2013).

[79] M. P. Zaletel, R. S. K. Mong, C. Karrasch, J. E. Moore, and F. Pollmann, Time-evolving a matrix product state with long-ranged interactions, Phys. Rev. B **91**, 165112 (2015).

[80] M. A. Nielsen and I. L. Chuang, *Quantum Computation and Quantum Information* (Cambridge University Press, Cambridge, UK, 2000).

[81] E. Knill, D. Leibfried, R. Reichle, J. Britton, R. B. Blakestad, J. D. Jost, C. Langer, R. Ozeri, S. Seidelin, and D. J. Wineland, Randomized benchmarking of quantum gates, Phys. Rev. A **77**, 012307 (2008).

[82] E. Magesan, J. M. Gambetta, and J. Emerson, Scalable and Robust Randomized Benchmarking of Quantum Processes, Phys. Rev. Lett. **106**, 180504 (2011).

[83] Y. Li, X. Chen, and M. P. A. Fisher, Quantum Zeno effect and the many-body entanglement transition, Phys. Rev. B **98**, 205136 (2018).

[84] M. J. Gullans and D. A. Huse, Dynamical Purification Phase Transition Induced by Quantum Measurements, Phys. Rev. X **10**, 041020 (2020).

[85] S. Sharma, X. Turkeshi, R. Fazio, and M. Dalmonte, Measurement-induced criticality in extended and long-range unitary circuits, SciPost Phys. Core **5**, 023 (2022).

[86] A. Lavasani, Y. Alavirad, and M. Barkeshli, Measurement-induced topological entanglement transitions in symmetric random quantum circuits, Nat. Phys. **17**, 342 (2021).

[87] O. Lunt, M. Szyniszewski, and A. Pal, Measurement-induced criticality and entanglement clusters: A study of one-dimensional and two-dimensional Clifford circuits, Phys. Rev. B **104**, 155111 (2021).

[88] S. Aaronson and D. Gottesman, Improved simulation of stabilizer circuits, Phys. Rev. A **70**, 052328 (2004).

[89] S. Anders and H. J. Briegel, Fast simulation of stabilizer circuits using a graph-state representation, Phys. Rev. A **73**, 022334 (2006).

[90] D. Gottesman, The heisenberg representation of quantum computers, arXiv:quant-ph/9807006.

[91] Note that this expression differs from the usual Heisenberg picture where the order of $\mathcal{U}$ and $\mathcal{U}^\dagger$ is reversed.

[92] See Supplemental Material at http://link.aps.org/supplemental/10.1103/PhysRevResearch.5.L012031 for details on the structure of the Clifford group, additional numerical results on transport, operator spreading, and entanglement growth in circuits with and without $U(1)$ symmetry in one and two dimensions, and entanglement dynamics in a long-range Ising chain, which includes Refs. [93,94].

[93] A. D. Córcoles, J. M. Gambetta, J. M. Chow, J. A. Smolin, M. Ware, J. D. Strand, B. L. T. Plourde, and M. Steffen, Process verification of two-qubit quantum gates by randomized benchmarking, Phys. Rev. A **87**, 030301(R) (2013).

[94] R. Koenig and J. A. Smolin, How to efficiently select an arbitrary Clifford group element, J. Math. Phys. **55**, 122202 (2014).

[95] R. Metzler and J. Klafter, The random walk's guide to anomalous diffusion: A fractional dynamics approach, Phys. Rep. **339**, 1 (2000).

[96] V. Zaburdaev, S. Denisov, and J. Klafter, Lévy walks, Rev. Mod. Phys. **87**, 483 (2015).

[97] D. Fattal, T. S. Cubitt, Y. Yamamoto, S. Bravyi, and I. L. Chuang, Entanglement in the stabilizer formalism, arXiv:quant-ph/0406168.

[98] Note that if one were to simulate the dynamics of a state stabilized by $\pm Z_\ell$ on all lattice sites, i.e., a product state $|\uparrow\downarrow\cdots\rangle$ in the Z basis, evolution with respect to Z-conserving Clifford gates would be entirely classical with $S(t)=0$ for all t's. This is in contrast to Haar-random gates with $U(1)$ symmetry.

[99] We emphasize again that this corresponds to 1d Hamiltonian systems with couplings $J\propto r^{-\alpha'}$ with $\alpha'=\alpha/2$.

[100] P. Zanardi, Entanglement of quantum evolutions, Phys. Rev. A **63**, 040304(R) (2001).

[101] S. Xu and B. Swingle, Scrambling dynamics and out-of-time ordered correlators in quantum many-body systems: A tutorial, arXiv:2202.07060.

[102] A. Hamma, R. Ionicioiu, and P. Zanardi, Bipartite entanglement and entropic boundary law in lattice spin systems, Phys. Rev. A **71**, 022315 (2005).

[103] Note that the rank has to be calculated by treating the entries ν_ℓ^i, μ_ℓ^i of $\mathcal{M}$ as elements of the field $\mathbb{F}_2$, i.e., addition and multiplication are performed mod 2.

[104] In fact, we find the closest agreement with $z=2$ if we make the ansatz $S(t)\sim t^{1/z}(\log t)^{2/3}$, from which we obtain $z=1.98(1)$.

[105] E. Leviatan, F. Pollmann, J. H. Bardarson, D. A. Huse, and E. Altman, Quantum thermalization dynamics with matrix-product states, arXiv:1702.08894.

[106] B. Ye, F. Machado, C. D. White, R. S. K. Mong, and N. Y. Yao, Emergent Hydrodynamics in Nonequilibrium Quantum Systems, Phys. Rev. Lett. **125**, 030601 (2020).

[107] T. K. Kvorning, L. Herviou, and J. H. Bardarson, Time-evolution of local information: Thermalization dynamics of local observables, SciPost Phys. **13**, 080 (2022).

[108] C. W. von Keyserlingk, F. Pollmann, and T. Rakovszky, Operator backflow and the classical simulation of quantum transport, Phys. Rev. B **105**, 245101 (2022).

[109] T. Farshi, J. Richter, D. Toniolo, A. Pal, and L. Masanes, Absence of localization in two-dimensional Clifford circuits, arXiv:2210.10129.

[110] A. Chandran and C. R. Laumann, Semiclassical limit for the many-body localization transition, Phys. Rev. B **92**, 024301 (2015).

[111] U. Agrawal, A. Zabalo, K. Chen, J. H. Wilson, A. C. Potter, J. H. Pixley, S. Gopalakrishnan, and R. Vasseur, Entanglement and Charge-Sharpening Transitions in $U(1)$ Symmetric Monitored Quantum Circuits, Phys. Rev. X **12**, 041002 (2022).

[112] Y. Bao, S. Choi, and E. Altman, Symmetry enriched phases of quantum circuits, Ann. Phys. (NY) **435**, 168618 (2021).

[113] S. Zhou, Z.-C. Yang, A. Hamma, and C. Chamon, Single T gate in a Clifford circuit drives transition to universal entanglement spectrum statistics, SciPost Phys. **9**, 087 (2020).

[114] D. Wei, A. Rubio-Abadal, B. Ye, F. Machado, J. Kemp, K. Srakaew, S. Hollerith, J. Rui, S. Gopalakrishnan, N. Y. Yao, I. Bloch, and J. Zeiher, Quantum gas microscopy of Kardar-Parisi-Zhang superdiffusion, Science **376**, 716 (2022).

[115] R. Islam, R. Ma, P. M. Preiss, M. Eric Tai, A. Lukin, M. Rispoli, and M. Greiner, Measuring entanglement entropy in a quantum many-body system, Nature (London) **528**, 77 (2015).

[116] N. M. Linke, S. Johri, C. Figgatt, K. A. Landsman, A. Y. Matsuura, and C. Monroe, Measuring the Rényi entropy of a two-site Fermi-Hubbard model on a trapped ion quantum computer Phys. Rev. A **98**, 052334 (2018).